Learning with Memory-based Virtual Classes for Deep Metric Learning

Supplementary Material

Contents

A. Loss Functions

In this section, we briefly describe softmax variant and proxy-based losses used in our study, as well as the hyper-parameters of each loss. For notation, we refer to the embedding features as x_i and corresponding label as y_i. Each loss function $l(\cdot)$ is written based on the generalized from of objective function:

$$\mathcal{L}(X, W) = -\frac{1}{\mid X \mid} \sum_{i=1}^{\mid X \mid} l(x_i, y_i), \tag{i}$$

where X and W are sets of embedding features and class weights, respectively.

Proxy-NCA [19] Typically, pair-based losses suffer from sampling issues such that sampling tuples heavily affects the training convergence. To address this problem, Proxy-NCA loss introduces class proxies, which represent each class. In this way, we can sample only one anchor and compare it against the corresponding positive and negative class proxies. It is noteworthy that class proxies have the same meaning as class weights from the softmax variants theoretically and practically; thus, we use the term 'class weights' to include class representatives or proxies in this paper. The Proxy-NCA loss can be formulated as:

$$l_{proxy-NCA}(x_i, y_i) = \log \frac{e^{-d(x_i, W_{y_i})}}{\sum_{j=1}^{C} e^{-d(x_i, W_j)}}, \tag{ii}$$

where $d(a, b) = \| a - b \|_2$ is the Euclidean distance between a and b.

Proxy-anchor [11] Unlike typical softmax variants and proxy-based losses, Proxy-anchor loss uses each proxy as an anchor and considers its relations with all samples in a batch. We define X_w^+ and X_w^- as the set of positive and negative embedding features of each proxy (class weight) w, respectively, and W^+ as the set of positive proxies of data in the mini-batch. Because of its peculiar structure, we formulate the Proxy-anchor loss based on the mini-batch as follows:

$$\mathcal{L}_{proxy-anchor}(X, W) = \frac{1}{\mid W^+ \mid} \sum_{w \in W^+} \log \left\{ 1 + \sum_{x \in X_w^+} e^{-\gamma(s(x,w)-\delta)} \right\} + \frac{1}{\mid W \mid} \sum_{w \in W} \log \left\{ 1 + \sum_{x \in X_w^-} e^{\gamma(s(x,w)+\delta)} \right\}, \tag{iii}$$

where $s(a, b) = a^T b$ denotes the cosine similarity between a and b, γ is a scaling factor, and δ is a margin parameter. We use $\gamma = 46$ and $m = 0.1$ for our hyper-parameters.

CosFace [30] CosFace loss reformulates the softmax loss as a cosine loss by l_2 normalizing the embedding features and class weights, which is equivalent to the Norm-softmax loss, and defines a decision margin in cosine space as:

$$l_{cosface}(x_i, y_i) = \log \frac{e^{\gamma(\cos(\theta_{y_i})-m)}}{e^{\gamma(\cos(\theta_{y_i})-m)} + \sum_{j=1, j \neq y_i}^{C} e^{\gamma \cos \theta_j}}, \tag{iv}$$

where γ is a scale and m is a margin parameter. For our hyper-parameters, we use $\gamma = 28$ and $m = 0.1$.

ArcFace [2] Similar to CosFace loss, ArcFace loss transforms the Norm-softmax loss function by applying an angular margin between the embedding x_i and the corresponding class weight W_{y_i} for each class. ArcFace loss can be formulated as:

$$l_{arcface}(x_i, y_i) = \log \frac{e^{\gamma \cos(\theta_{y_i}+m)}}{e^{\gamma \cos(\theta_{y_i}+m)} + \sum_{j=1, j \neq y_i}^{C} e^{\gamma \cos \theta_j}}, \tag{v}$$

where we use the scale $\gamma = 24$ and the margin $m = 0.1$.

CurricularFace [7] CurricularFace incorporates the idea of curriculum learning into the ArcFace loss to adjust the relative importance of easy and hard samples during training. The loss function of CurricularFace is formulated as follows:

$$l_{curricularface}(x_i, y_i) = \log \frac{e^{\gamma T(\cos\theta_{y_i})}}{e^{\gamma T(\cos\theta_{y_i})} + \sum_{j=1, j\neq y_i}^{C} e^{\gamma N(t, \cos\theta_j)}}, \tag{vi}$$

$$T(cos\theta_{y_i}) = cos(\theta_{y_i} + m), \tag{vii}$$

$$N(t, cos\theta_{y_j}) = \begin{cases} cos\theta_{y_j}, & T(cos\theta_{y_i}) - cos\theta_j \geq 0 \\ cos\theta_{y_j}(t^{(k)} + cos\theta_j), & T(cos\theta_{y_i}) - cos\theta_j < 0, \end{cases} \tag{viii}$$

where $T(\cdot)$ and $N(\cdot)$ are modulation functions for the positive and negative cosine similarities, respectively. The parameter $t^{(k)}$ of the k-th step is computed as follows:

$$t^{(k)} = \alpha r^{(k)} + (1-\alpha)t^{(k)}, \tag{ix}$$

where $r^{(k)}$ is the average of the positive cosine similarities and α is the momentum parameter. For our hyper-parameters, we use $\alpha = 0.99$, $\gamma = 26$ and $m = 0.3$.

B. Details of MemVir

B.1. Proof of Gradient Analysis for Generalization

We provide a detailed proof of gradient analysis for generalization, which is discussed in Section 3.3.3. The proof is shown by comparing the gradient descent of softmax and MemVir.

Gradient Descent of Softmax: As mentioned in Equation 6 of the main paper, the softmax loss can be written as follows:

$$l_{softmax}(x_i, y_i) = \log \frac{e^{\alpha(x_i, y_i)}}{\sum_{j=1}^{C} e^{\alpha(x_i, j)}}, \tag{x}$$

where $\alpha(x_i, j) = W_j^T x_i$. The gradient of the softmax loss over the embedding feature x_i can be inducted as follows:

$$\begin{aligned} \frac{\partial l_{softmax}(x_i, y_i)}{\partial x_i} &= \frac{\sum_{j=1}^{C} e^{\alpha(x_i,j)}}{e^{\alpha(x_i,y_i)}} \frac{W_{y_i} e^{\alpha(x_i,y_i)} \sum_{j=1}^{C} e^{\alpha(x_i,j)} - e^{\alpha(x_i,y_i)} \sum_{j=1}^{C} W_j e^{\alpha(x_i,j)}}{(\sum_{j=1}^{C} e^{\alpha(x_i,j)})^2} \\ &= W_{y_i} - \frac{\sum_{j=1}^{C} e^{\alpha(x_i,j)} W_j}{\sum_{j=1}^{C} e^{\alpha(x_i,j)}}. \end{aligned} \tag{xi}$$

For a moderately-trained model, x_i should much more closer to W_{y_i} compared to W_j for $j \neq y_i$, which leads to $\alpha(y_i, i) > \alpha(j, i)$ (*Condition 1*). Besides, for a model with norm-softmax loss, $\alpha(j, i) \in (-\gamma, +\gamma)$, where $\gamma \geq 10$ in our experiment setting (*Condition 2*). Considering *Condition 1* with *Condition 2* together, we can derive the conclusion that $e^{\alpha(x_i,y_i)} >> e^{\alpha(x_i,j)}$ for $j \neq y_i$. By applying such conclusion to the numerator of Equation xi for approximation, following equation can be achieved:

$$\begin{aligned} \frac{\partial l_{softmax}(x_i, y_i)}{\partial x_i} &= W_{y_i} - \frac{\sum_{j=1}^{C} e^{\alpha(x_i,j)} W_j}{\sum_{j=1}^{C} e^{\alpha(x_i,j)}} \\ &\approx W_{y_i} - \frac{e^{\alpha(x_i,y_i)} W_{y_i}}{\sum_{j=1}^{C} e^{\alpha(x_i,j)}} \\ &= \tau W_{y_i}, \end{aligned} \tag{xii}$$

$$\tau = 1 - \frac{e^{\alpha(x_i,y_i)}}{\sum_{j=1}^{C} e^{\alpha(x_i,j)}}. \tag{xiii}$$

It is obvious that $\tau > 0$. Besides, when $x_i \to W_{y_i}$, $e^{\alpha(x_i,y_i)}$ becomes much larger than $e^{\alpha(x_i,j)}$, which leads to $\tau = 1 - \frac{e^{\alpha(x_i,y_i)}}{\sum_{j=1}^{C} e^{\alpha(x_i,j)}} \to 1 - \frac{e^{\alpha(x_i,y_i)}}{e^{\alpha(x_i,y_i)}} = 0$, implying that x_i converges as close to W_{y_i} as possible. This can result in a strong focus on the target weight W_{y_i} and an over-fit to the seen classes of the training data.

Gradient Descent of MemVir: For MemVir, the softmax function in Equation x should be re-written as follows:

$$l_{softmax}(x_i, y_i) = \log \frac{e^{\alpha(x_i,y_i)}}{\sum_{j=1}^{(N+1)C} e^{\alpha(x_i,j)}}, \tag{xiv}$$

where the number of class weights increase from C to $(N+1)C$ compared to softmax because of the existence of the virtual classes. Then, the gradient of MemVir + softmax loss over the embedding feature x_i can be inducted as follows:

$$\begin{aligned} \frac{\partial l_{MemVir}(x_i, y_i)}{\partial x_i} &= \frac{\sum_{j=1}^{(N+1)C} e^{\alpha(x_i,j)}}{e^{\alpha(x_i,y_i)}} \frac{W_{y_i} e^{\alpha(x_i,y_i)} \sum_{j=1}^{(N+1)C} e^{\alpha(x_i,j)} - e^{\alpha(x_i,y_i)} \sum_{j=1}^{(N+1)C} W_j e^{\alpha(x_i,j)}}{(\sum_{j=1}^{(N+1)C} e^{\alpha(x_i,j)})^2} \\ &= W_{y_i} - \frac{\sum_{j=1}^{(N+1)C} e^{\alpha(x_i,j)} W_j}{\sum_{j=1}^{(N+1)C} e^{\alpha(x_i,j)}} \end{aligned} \tag{xv}$$

During training process, the class weights of past and present tend to be close each other, leading to the conclusion of $e^{\alpha(x_i,y_i)} >> e^{\alpha(x_i,j)}$ for $j \neq y_i^{(n)}$, where $y_i^{(n)}$ with $n = 1, 2, 3, ..., N$ represents the virtual classes of class y_i from the step n and the term $y_i^{(0)} = y_i$ is used for convenience. By applying such conclusion to the numerator of Equation xv for approximation, following equation can be achieved:

$$\begin{aligned} \frac{\partial l_{MemVir}(x_i, y_i)}{\partial x_i} &= W_{y_i} - \frac{\sum_{j=1}^{(N+1)C} e^{\alpha(x_i,j)} W_j}{\sum_{j=1}^{(N+1)C} e^{\alpha(x_i,j)}} \\ &\approx W_{y_i} - \frac{\sum_{n=0}^{N} e^{\alpha(x_i,y_i^{(n)})} W_{y_i^{(n)}}}{\sum_{j=1}^{(N+1)C} e^{\alpha(x_i,j)}} \\ &= \tau_0 W_{y_i} + \sum_{n=1}^{N} \tau_n W_{y_i^{(n)}}, \end{aligned} \tag{xvi}$$

$$\tau_0 = 1 - \frac{e^{\alpha(x_i,y_i)}}{\sum_{j=1}^{(N+1)C} e^{\alpha(x_i,j)}}, \tau_n = -\frac{e^{\alpha(x_i,y_i^{(n)})}}{\sum_{j=1}^{(N+1)C} e^{\alpha(x_i,j)}} \tag{xvii}$$

It is obvious that $\tau_0 > 0$. However, τ_0 would not be close to zero whether x_i is nearby W_{y_i} or not, because virtual classes would be close to W_{y_i}. This can alleviate the phenomenon of the embedding feature becoming extremely close to the target W_{y_i}. In addition, because of τ_n, such alleviation would be more extensive and can effectively ease the intense focus of the softmax loss, leading to a more substantial generalization.

B.2. Revisiting Slow Drift Phenomena

"*Slow drift*" phenomena have been introduced in [33], which identifies the slow drifting speed of the embeddings by measuring the difference of features for the same instance computed at different training steps. With this observation, [33] suggests using the embeddings of past steps for loss computation of the current step. We reproduce "*slow drift*" phenomena with weight features as follows:

$$\triangle d(W_t, W_{t-m}) := \| W_t - W_{t-(m+1)} \|_2^2, \tag{xviii}$$

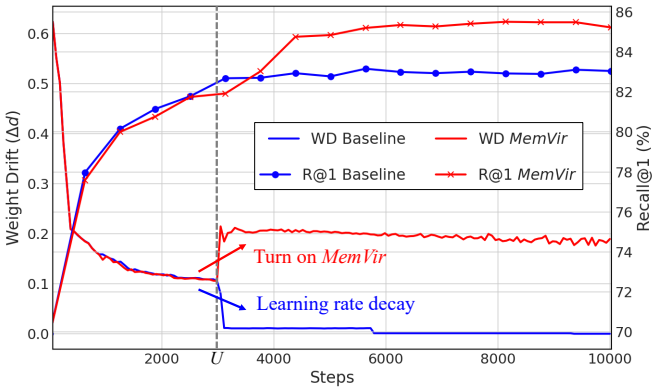

Figure A. Weight drift $\triangle d$ with $m = 100$ and corresponding Recall@1 performance of baseline and MemVir(1,100).

where W_t is weight features of current step t and $W_{t-(m+1)}$ is weight features of past step $t-(m+1)$. As illustrated in Figure A, the weight drift of the baseline is very slow, especially after learning rate decay. We can observe that it converges to local minima with a negligible amount of weight updates after the learning rate decay. On the contrary, when we turn on MemVir instead of learning rate decay, we observe that the weight drift has risen by the enlarged magnitude of gradient; thus, it gives more chance to escape from the local minima for performance improvement.

We further analyze these phenomena by comparing the gradient descent of the softmax loss and MemVir. The softmax loss can be written as follows:

$$\begin{aligned} l_{softmax}(x_i, y_i) &= \log \frac{e^{W_{y_i}^T x_i}}{\sum_{j=1}^{C} e^{W_j^T x_i}} \\ &= \log \frac{e^{\alpha(y_i,i)}}{\sum_{j=1}^{C} e^{\alpha(j,i)}}, \end{aligned} \tag{xix}$$

where $\alpha(j,i) = W_j^T x_i$. Then, the gradient of such loss over $\alpha(j,i)$ can be inducted as follows:

$$\begin{aligned} \frac{\partial l_{softmax}(x_i, y_i)}{\partial \alpha(y_i, i)} &= \frac{\sum_{j=1}^{C} e^{\alpha(j,i)} - e^{\alpha(y_i,i)}}{\sum_{j=1}^{C} e^{\alpha(j,i)}} \\ &= 1 - \frac{e^{\alpha(y_i,i)}}{\sum_{j=1}^{C} e^{\alpha(j,i)}}. \end{aligned} \tag{xx}$$

Because $e^{\alpha(y_i,i)} >> e^{\alpha(j,i)}$ for $j \neq y_i$, thus, $\frac{\partial l_{softmax}(x_i,y_i)}{\partial \alpha(y_i,i)}$ is close to zero. Considering the weight update is performed by $w = w - \eta \frac{\partial L}{\partial w}$, where η is a learning rate, the weight update will be negligible and result in "*slow drift*" phenomena, especially with a small learning rate.

MemVir overcomes such situation by increasing the magnitudes of gradients. The inducted gradient of MemVir over $\alpha(j,i)$ is as follows:

$$\begin{aligned} \frac{\partial l_{softmax}(x_i, y_i)}{\partial \alpha(y_i, i)} &= \frac{\sum_{j=1}^{(N+1)C} e^{\alpha(j,i)} - e^{\alpha(y_i,i)}}{\sum_{j=1}^{(N+1)C} e^{\alpha(j,i)}} \\ &= 1 - \frac{e^{\alpha(y_i,i)}}{\sum_{j=1}^{(N+1)C} e^{\alpha(j,i)}} \\ &\approx 1 - \frac{e^{\alpha(y_i,i)}}{e^{\alpha(y_i,i)} + \sum_{n=1}^{N} e^{\alpha(y_i^{(n)},i)}}, \end{aligned} \tag{xxi}$$

	Softmax	ArcFace	CurricularFace
CARS196	(30, 50)	(40,50)	(5,100)
SOP	(4, 50)	(10,50)	(9,50)

(a) Comparison with related methods.

	Softmax	Norm-softmax	CosFace	ArcFace	Proxy-NCA	Proxy-anchor
CUB200	(5,75)	(10,10)	(25,150)	(40,40)	(10,25)	(5,75)
CARS196	(15,25)	(45,10)	(25,150)	(15,10)	(20,25)	(15,75)
SOP	(3,150)	(7,90)	(6,100)	(9,80)	(2,80)	(8,50)

(b) Conventional evaluation.

	Norm-softmax	CosFace	ArcFace	Proxy-NCA	Proxy-anchor
CUB200	(15,20)	(35,75)	(40,100)	(40,50)	(15,75)
CARS196	(50,50)	(2,300)	(35,10)	(10,250)	(25,25)
SOP	(15,50)	(10,50)	(5,200)	(20,50)	(5,100)

(c) MLRC evaluation.

Table A. Hyper-parameters (N,M) of MemVir for each experiment.

where $y_i^{(n)}$ is the index of the weights before n steps. As $e^{\alpha(y_i^{(n)},i)}$ are not close to zero, $\frac{\partial l_{softmax}(x_i,y_i)}{\partial \alpha(y_i,i)}$ will not be close to zero. Thus, the gradient of MemVir will be relatively larger than that of the softmax loss, which gives more chance to escape from the local minima. Note that the magnitudes of gradients can be controlled by the difficulty of curriculum learning, such as hyper-parameters N and M.

C. Details of Experimental Settings

C.1. Datasets

Throughout the paper, we use three famous benchmarking datasets in deep metric learning (DML) as follows:

- CUB200-2011 (CUB200) [28]: CUB200 contains 11,788 images of birds in 200 classes. We use 5,864 images of the first 100 classes for training and 5,924 images of the other 100 classes for testing without bounding box information.
- CARS196 [16]: CARS196 contains 16,185 images of cars in 196 classes. We use 8,054 images of the first 98 classes for training and 8,131 images of the other 98 classes for testing without bounding box information.
- Standford Online Products (SOP) [21]: SOP contains 120,053 images of products in 22,634 classes. We use 59,551 images of the 11,318 classes for training and 60,502 images of the other 11,316 classes for testing.

C.2. Implementation

We implement all models using the PyTorch framework [23], and experiments are performed on Nvidia V100 GPUs. For the *conventional evaluation*, we follow the widely used training and testing protocol as [21, 25, 11, 31]. For the *Metric Learning Reality Check (MLRC) evaluation*, we follow the training and evaluation procedure defined in [20].

C.2.1 Conventional Evaluation

Input images are augmented by random cropping and horizontal flipping in the training phase, whereas they are center-cropped in the test phase. The size of the cropped images is 224×224. For the backbone network, the Inception network with batch normalization (BN-Inception) [9] pre-trained with ImageNet [1] is used. We use a global average pooling followed by a fully connected layer for dimensionality reduction and set the dimension of the embedding feature to 512. We freeze batch normalization for CUB200 and CARS196 and keep batch normalization training for SOP by following [24, 31, 11]. The batch size is set to 128 for every experiment. Optimization is performed using Adam optimizer [14] with a learning rate of 10^{-4} for CUB200 and CARS196, and 10^{-3} for SOP. The learning rate is decayed by a factor of 0.1 at the 50th epoch

for CARS196, and the 20th epoch for CUB200 and SOP. For MemVir, we use warm-up epoch $U_e = 50$ for CARS196 and SOP, and $U_e = 20$ for CUB200 without learning rate decay. With the same hyper-parameters of the baselines, we tune hyper-parameters N and M for MemVir via hyper-parameter search as described in A.

Proxy-anchor: For more details of Proxy-anchor loss in terms of implementation, we have found that proxy-anchor loss has been implemented with additional tricks, which is also mentioned in [36]. The additional tricks are as follows: 1) an AdamW optimizer [17] instead of Adam optimizer [14], 2) a parameter warm-up strategy for better optimization stability, 3) instead of an average pooling, a combination of an average and a max pooling following the backbone network. For a fair comparison, we discard those tricks and follow the conventional metric learning protocol in every experiment. Exceptionally, we use the parameter warm-up with one epoch for SOP dataset because the training with Proxy-anchor loss fails without the parameter warm-up strategy.

Multi-Similarity loss: In Multi-Similarity (MS) loss [31], we have found that the best scores reported in the paper are conducted with either too small or large batch size, such as a batch size of 80 for CUB200 and batch size of 1000 for SOP. For a fair comparison, we conduct experiments of MS loss with the conventional batch size of 128., including the number of instances of 4. Note that we use the number of instances of 4 instead of 5 from the paper because 128 is not divisible by 5.

C.2.2 MLRC Evaluation

Each image is resized to make its shorter side to be the length of 256, then augmented by random cropping to have a size between 40 and 256, and by aspect ratio between 3/4 and 4/3 in the training phase. The resulting image is then resized to 227×227 and flipped horizontally with a 50% probability. In the test phase, each image is resized to 256 and center-cropped to 227. We use BN-Inception for the backbone network with an output embedding size of 128. Optimization is performed using RMSprop optimizer with a learning rate of 10^{-6} and a batch size of 32. To find the best hyper-parameters for loss functions, we run 50 experiments of hyper-parameter search with 4-fold cross-validation of each experiment. With the best hyper-parameters found, we conduct 10 training runs and report the average and confidence intervals to be less subject to random seed noise. We report both separated (128-dim) and concatenated (512-dim) performance, where the 512-dim embedding is concatenated and l_2-normalized of 128-dim embedding of the 4 models.

C.3. fANOVA

We apply the fANOVA [8] analysis framework to estimate the impact of each hyper-parameter on the performance of MemVir in Section 4.4 and D.5. fANOVA predicts the marginal performance using a predictive model (random forest), which is a function of the model's hyper-parameters. Then, it determines the extent to which each hyper-parameter or pair-wise interaction contributes to the model performance. In the experiments of MemVir, we conduct 5 training runs for each pair of (N, M), and each pair is created by the combination of range N and range M. For CUB200 and CAS196, range N is 5 to 50 in 5 intervals including 1, and range M is 0 to 100 in 10 intervals. For SOP, we reduce the range N to be 1 to 7 because of memory limitation of one gpu. These experimental results are used to train random forests for fANOVA analysis.

D. Extended Experiments

D.1. Analysis of Memory and Computational Cost

In this section, we analyze memory and computational cost of MemVir with the same experimental setting described in Section C.2.1. MemVir requires $O(BNM(D + C))$ for the memory queues, $O(BCN^2)$ for the similarity matrix, and $O(BCN^2)$ for the computational complexity during the training phase, where B, C, and D are batch size, number of classes, and feature dimension, respectively. In the inference phase, MemVir requires no additional memory or computational cost. As shown in Figure B, the memory usage of MemVir with 128 batch size increases as N and M are increased. Compared to the Norm-softmax model, MemVir(1,100) and MemVir(45,10) improve $+1.3\%$ and $+3.5\%$ performances with additional $52MB$ and $704MB$ GPU memory, respectively. MemVir(50,100), which increases the number of classes and embeddings by 50 times, only requires additional 2.9GB GPU memory and shows better memory efficiency than the baseline with 256 batch size, which requires 6.8GB more GPU memory than MemVir(50,100) with 128 batch size. Even though the memory usage of MemVir would be larger for datasets with a large number of classes, it can be controlled by placing a reduced number of class weights in $\mathbb{W}$, which are corresponding classes of current step embeddings. In terms of performance, applying MemVir is more effective than increasing the batch size, which is empirically shown in Section 4.3.

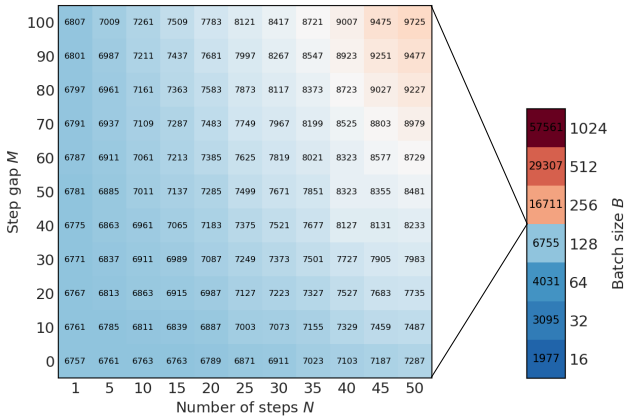

(a) *MemVir(N,M)* + Norm-softmax with 128 batch size (b) Norm-softmax

Figure B. Memory usage (MB) of MemVir(N,M) + Norm-softmax with 128 batch size and Norm-softmax with different batch size on CARS196 dataset.

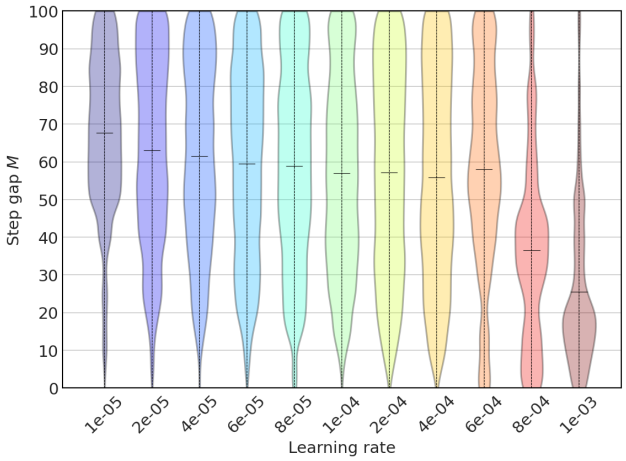

Figure C. Distributions of relative performances for each learning rate by step gap M. For each learning rate, Recall@1 performances of MemVir(1,M) on CARS196 dataset are normalized across step gap M.

D.2. Impact of Learning Rate

Typically, memory-based methods [13, 33] get influenced by learning rate because it affects the difference between training steps. As discussed in Section 3.2, MemVir can control the difference between training steps with margin parameter M. To see the impact of learning rate, we train MemVir(1,M) with a range M from 0 to 100 in 5 intervals and normalize Recall@1 performances across step gap M for each learning rate. We plot the distributions of relative performances by step gap M for each learning rate. As described in Figure C, the larger learning rate requires the smaller step gap M for better performance. This is because a sufficient difference between the training steps can be achieved by a large gap M for a small learning rate and a small gap M for a large learning rate. Thus, the different learning rates can be controlled by the step gap M for MemVir.

D.3. Impact of Warm-up

As discussed in Section 3.3.1, the warm-up period of MemVir enables the model to avoid training with distractive virtual classes from the initial step. To see the impact of the warm-up period, we conduct experiments by differentiating the warm-up epoch with MemVir(1,100) and MemVir(50,10). As shown in Figure D, MemVir(1,100) shows the lowest performance when $U_e = 0$ and stable performance for $U_e > 0$. For MemVir(50,10), the lowest performance is also shown when $U_e = 0$ and the performance increases until $U_e = 60$, then decreases. It is noteworthy that the lowest performance of MemVir with $U_e = 0$ still shows higher performance than that of the baseline. The results show that proper steps of warm-up help increase the capability of MemVir, and this pattern stands out more to MemVir with longer scheduling of virtual classes addition.

D.4. Robustness to Input Deformation

We now evaluate the quality of representations learned with MemVir with respect to generalization to input deformations. We train models with Norm-softmax loss and MemVir + Norm-softmax loss on CARS196 dataset but test them on the novel (not seen during training) input deformations of the test set. For the input deformation, we use the *imgaug* [10] python library and the details of deformations are as follows.

- *Cutout*: Each image is randomly filled with two gray pixels that are 20% of the image size.
- *Dropout*: p% of pixels are dropped from each image, where p is randomly sampled from a range $0\% \leq p \leq 20\%$.
- *Zoom-in* and *zoom-out*: Each image is transformed by zoom-in and zoom-out with scale of 50% and 150%, respectively.
- *Rotation* and *shearing*: Each image is transformed by rotation and shearing with a randomly sampled degree between -30° and 30°.

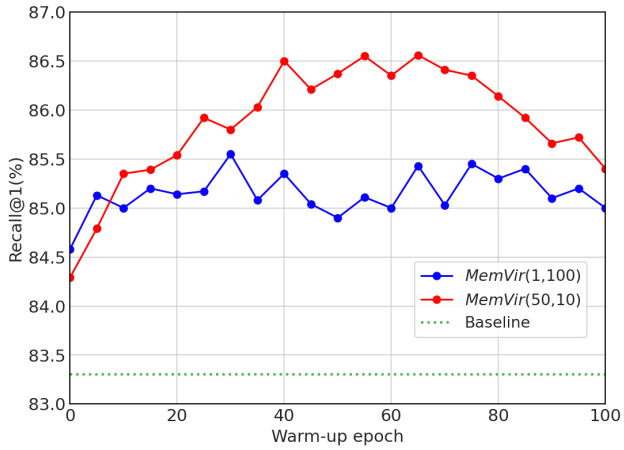

Figure D. Impact of warm-up epoch U_e of MemVir + Norm-softmax on CARS196 dataset. We report the performance of MemVir with different warm-up epoch. Note that the performance of baseline Norm-softmax is unrelated to the warm-up epoch.

Deformation	Norm-softmax	*MemVir*
W/o deformation	83.3	86.6 (+3.3)
Cutout	75.3	79.2 (+3.9)
Dropout	59.7	67.7 (+8.0)
Zoom in	64.3	68.1 (+3.9)
Zoom out	78.3	81.7 (+3.4)
Rotation	70.8	73.4 (+2.6)
Shearing	70.3	73.2 (+3.0)
Gaussian noise	65.1	71.2 (+6.1)
Gaussian blur	74.4	78.2 (+3.8)

Table B. Recall@1(%) performance of input deformations with CARS196 trained models. We compare Norm-softmax with MemVir(50,10) + Norm-softmax.

(N,M)	(0,0)-baseline	(1,100)	(5,100)	(10,100)	(20,100)
Only-weights	83.6	84.4	**84.5**	84.3	83.8
MemVir		84.9	85.1	85.5	**85.8**

Table C. Recall@1 (%) of only-weights and MemVir on CARS196.

- *Gaussian noise*: Gaussian noise is applied to each image, where the noise is sampled per pixel from a normal distribution $N(0, s)$ and s is sampled between 0 and 0.2×255.

- *Gaussian blur*: Gaussian kernel with a sigma of 3.0 is applied to each image.

As shown in Table B, performances of Norm-softmax are degraded significantly when applied input deformations. On the other hand, MemVir exhibits relatively smaller performance degradation compared to that of the Norm-softmax, and shows better robustness to all input deformations, particularly for dropout and gaussian noise. This demonstrates that MemVir allows the model to obtain a more generalized embedding space.

D.5. Impact of Hyper-parameters

In addition to the hyper-parameter analysis of CARS196 in Section 4.4, we include extra analyses on CUB200 and SOP. As shown in Figure E, the performance on CUB200 increases until the margin $M = 5$, and then decreases. For the margin, the performance improves as the margin M increases. In the case of SOP, the performance increases as both N and M increase while there is a slight degradation of performance around $M = 10$. As mentioned in Section 4.4, the performance pattern and importance of each hyper-parameter differs for each dataset because of different data characteristics. However, we can observe that, for both CUB200 and SOP, the best performance is achieved when N and M are larger than 1 and 0, respectively.

D.6. Impact of Embeddings and Class Weights in Virtual Class

To investigate the quantitative impact of embeddings and class weights in virtual classes, we conduct an experiment by using only class weights in virtual classes. Note that using only embeddings in virtual classes is not possible because every embedding requires corresponding class weights in loss computation. Table C shows that using only class weights increases performance than the baseline, but using both embeddings and class weights (MemVir) outperforms it. It suggests the necessity of embeddings to form proper virtual classes.

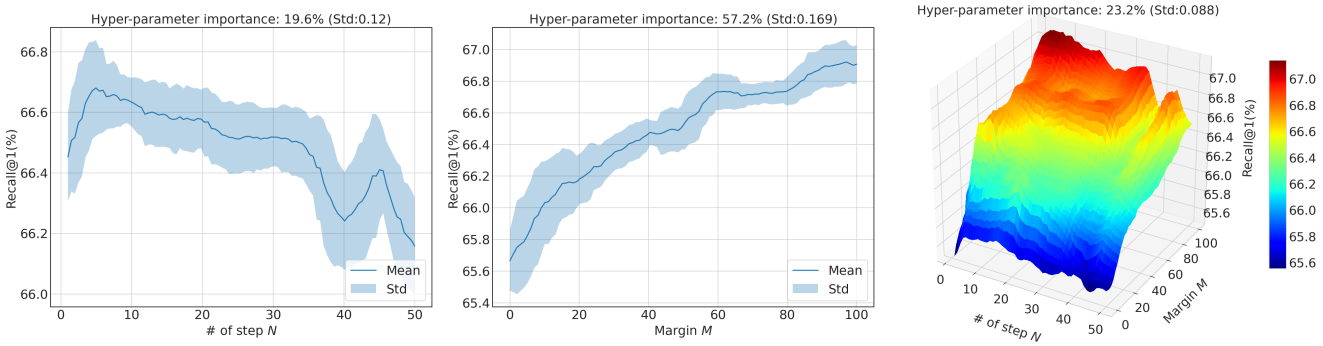

(a) Impact of number of step N (b) Impact of margin M (c) Impact of pair-wise interaction

Figure E. Impact of hyper-parameters on CUB200 with fANOVA analysis framework.

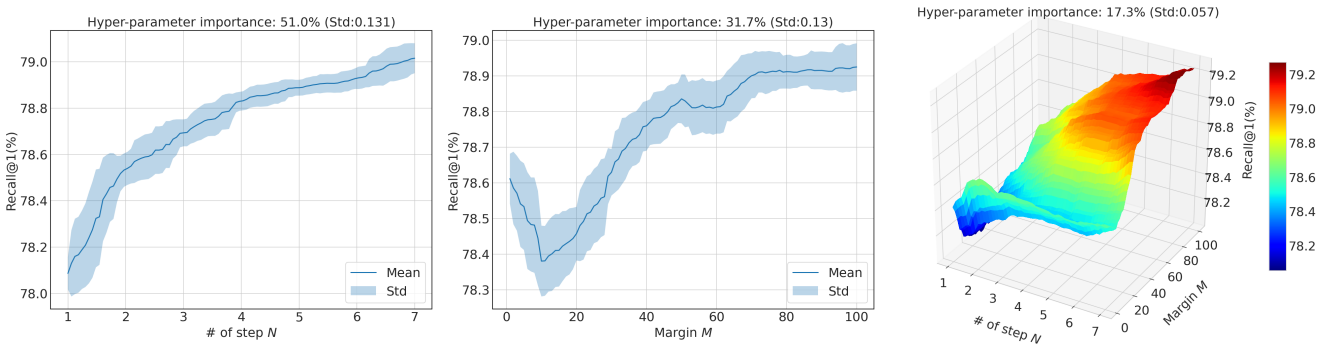

(a) Impact of number of step N (b) Impact of margin M (c) Impact of pair-wise interaction

Figure F. Impact of hyper-parameters on SOP with fANOVA analysis framework.

D.7. Comparison with Related Methods

We provide an extended comparison with related methods from image recognition tasks following Section 4.5. As shown in Table Da, we set two different experimental setups to compare the methods in various experimental settings. Setup 1 is following the experimental settings from BroadFace [13] and CurricularFace [7], and setup 2 is from the conventional DML settings described in Section C.2.1 with ResNet50 [6] backbone. As XBM [33] shares the memory-based idea with BroadFace, we conduct experiments of XBM in ArcFace loss to compare with BroadFace. As shown in Table D, Virtual softmax degrades the performance for both setups 1 and 2, whereas MemVir improves the performance for both setups. In Virtual softmax, the single virtual class weight is created by $W_{virt} = \frac{\|W_{y_i}\| X_i}{\|X_i\|}$. We observe that the logit with virtual class $W_{virt}^T X_i$ is much larger than the positive logit $W_{y_i}^T X_i$ due to the same direction of vectors W_{virt} and X_i, and it distracts the model from stable training. Combining XBM with ArcFace shows a little performance improvement for both setups, but we observe performance degradation when the memory size is large, as reported in BroadFace. To resolve this problem, BroadFace presents a compensation technique and gradient control. For the details, the compensation technique compensates memorized embeddings by considering class weights updating, while the gradient control computes the loss function into two ways: (1) loss from a mini-batch is for updating the backbone network. (2) loss from the mini-batch and past embeddings is for updating the class weights. BroadFace shows a higher performance boost with the SGD optimizer in setup 1 than the Adam optimizer in setup 2. We observe that BroadFace is sensitive to optimizer type, which could be because of the specifically designed gradient control. On the other hand, MemVir achieves larger performance gains for both setups without any modification of loss functions. CurricularFace shows competitive performance in both setups with an embedded curriculum learning process. When MemVir is applied, the performance of CurricularFace could further be improved by exploiting augmented information from virtual classes.

	Backbone	Dimension	Batch size	Optimizer	Initial LR
Setup 1	ResNet50	512	512	SGD	0.005
Setup 2	ResNet50	512	128	Adam	0.0001

(a) Two different experimental setups.

Method	CARS196				SOP			
	R@1	R@2	R@4	R@8	R@1	R@10	R@100	R@1000
Softmax	78.3	86.4	91.9	**95.7**	76.6	89.4	95.8	**98.8**
Virtual Softmax	75.1	84.1	90.1	94.0	74.5	87.9	94.8	98.3
MemVir + Softmax	**79.2**	**87.0**	**92.1**	**95.7**	**78.9**	**90.6**	**96.2**	**98.8**
ArcFace	78.8	86.4	91.7	95.4	76.9	89.1	95.0	98.2
XBM + ArcFace	78.9	86.2	91.9	95.5	78.1	89.7	95.8	98.2
BroadFace + ArcFace	79.5	87.3	92.0	95.5	80.2	91.0	95.9	98.4
MemVir + ArcFace	**80.7**	**88.1**	**92.7**	**95.8**	**80.8**	**91.3**	**96.5**	**98.9**
CurricularFace	79.9	87.3	92.0	95.6	79.8	90.7	95.6	98.2
MemVir + CurricularFace	**81.0**	**87.9**	**92.9**	**95.8**	**81.3**	**91.7**	**96.5**	**98.8**

(b) Performance (%) comparison in experimental setup 1.

Method	CARS196				SOP			
	R@1	R@2	R@4	R@8	R@1	R@10	R@100	R@1000
Softmax	82.4	88.8	92.1	95.2	78.1	89.1	95.2	97.9
Virtual Softmax	77.6	85.3	90.7	94.3	77.3	87.8	94.1	97.2
MemVir + Softmax	**86.8**	**92.3**	**95.5**	**97.6**	**78.9**	**90.6**	**96.2**	**98.8**
ArcFace	83.2	89.5	93.7	96.4	78.6	90.3	95.8	98.5
XBM + ArcFace	83.9	90.3	94.2	96.5	78.8	90.1	96.0	98.3
BroadFace + ArcFace	83.9	90.5	94.2	**96.9**	79.1	90.7	**96.2**	**98.8**
MemVir + ArcFace	**85.4**	**90.9**	**94.7**	**96.9**	**79.5**	**90.9**	**96.2**	**98.8**
CurricularFace	83.5	90.1	94.2	96.5	78.5	90.1	95.6	98.4
MemVir + CurricularFace	**85.4**	**91.0**	**94.5**	**96.9**	**79.3**	**90.5**	**95.8**	**98.5**

(c) Performance (%) comparison in experimental setup 2.

Table D. Performance (%) comparison with related methods in two different experimental setups.

D.8. Visualization of Embedding Space

For further understanding, we include extended t-SNE [18] visualization of embedding space, followed by Figure 6 in Section 4.2. As illustrated in Figure Ga, Gb, and Gc, embedding features from the seen classes are getting clustered by training process, and further training may cause a model overly fitted to the seen classes. To alleviate this strong focus on seen classes, MemVir begins to add virtual classes slowly and increases learning difficulty gradually, as described in Figure Gd, Ge, Gf, Gg and Gh. Actual and virtual classes, which are originated from the same class label, tend to be located close to each other. Further training allows the model to learn how to discriminate additional classes effectively, as illustrated in Figure Gi, Gj, Gk, and Gl. Finally, we obtain a model with sufficient discriminative power over all actual and virtual classes at the 200th epoch.

D.9. Comparison with State-of-the-art

This section includes extended comparison with state-of-the-art methods for both *conventional evaluation* and *MLRC evaluation* in addition to Section 4.6. As shown in Table E, G, and I of conventional evaluation, we report additional Recall@k performance and comparison with different types of DML methods. For MLRC evaluation, we report both separated (128-dim) and concatenated (512-dim) performance as presented in Table F, H, and J. In conventional evaluation, MemVir shows a significant performance boost in all Recall@k for every dataset and loss function. Compared with different types of DML methods, including ensemble, sample generation, memory-based, pair-based, proxy-based, and softmax variants,

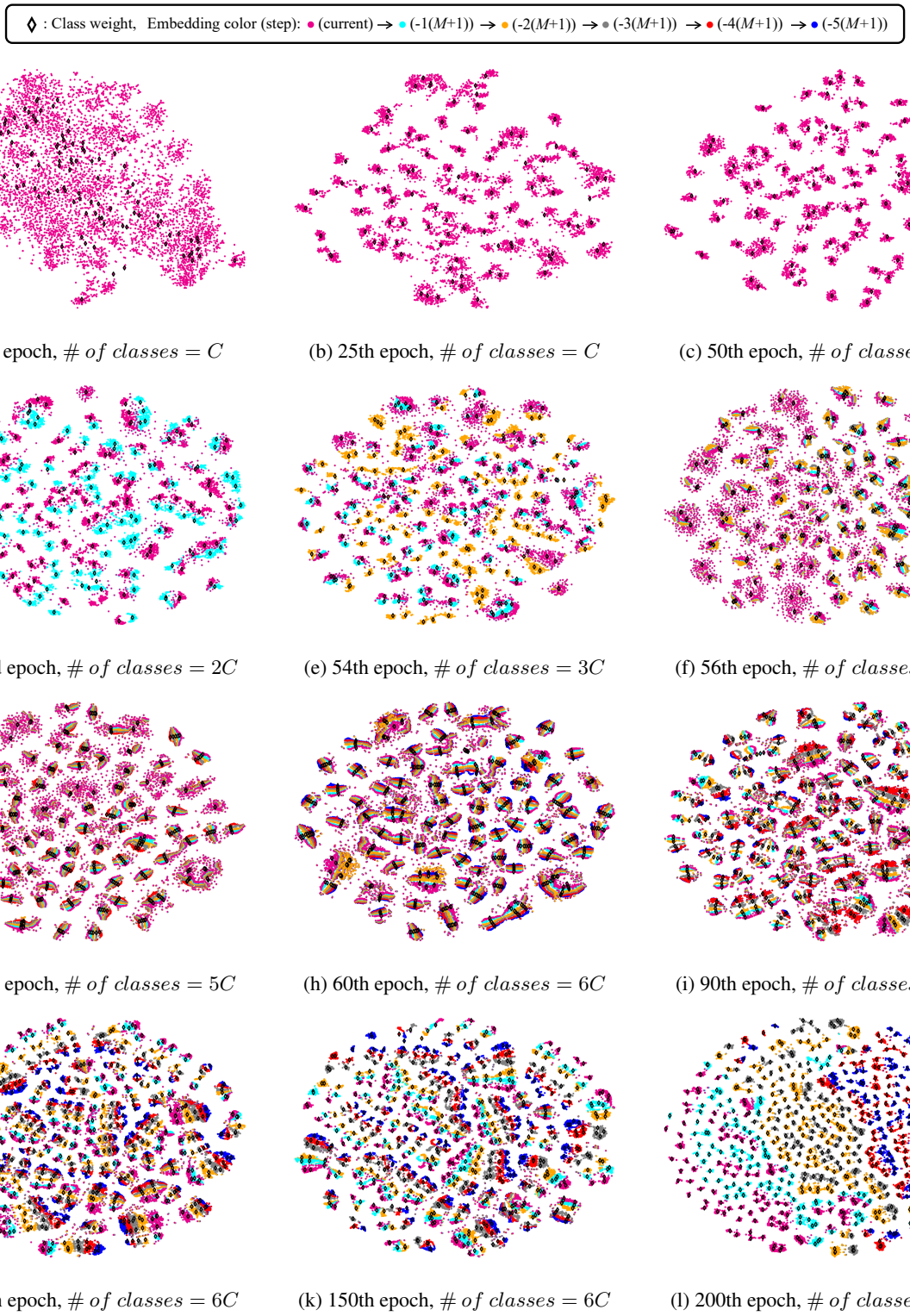

(a) 1st epoch, $\#\ of\ classes = C$ (b) 25th epoch, $\#\ of\ classes = C$ (c) 50th epoch, $\#\ of\ classes = C$

(d) 52nd epoch, $\#\ of\ classes = 2C$ (e) 54th epoch, $\#\ of\ classes = 3C$ (f) 56th epoch, $\#\ of\ classes = 4C$

(g) 58th epoch, $\#\ of\ classes = 5C$ (h) 60th epoch, $\#\ of\ classes = 6C$ (i) 90th epoch, $\#\ of\ classes = 6C$

(j) 120th epoch, $\#\ of\ classes = 6C$ (k) 150th epoch, $\#\ of\ classes = 6C$ (l) 200th epoch, $\#\ of\ classes = 6C$

Figure G. t-SNE visualization of 512-dimensional embedding space. Embedding features are extracted by a model trained with MemVir(5,100) on CARS196 training data. Each color indicates a step for embedding features.

MemVir shows competitive performance for all datasets. In MLRC evaluation, MemVir enjoys a high-performance gain over every dataset and loss function in both separated (128-dim) and concatenated (512-dim) experiments. Considering MLRC evaluation is designed for fair evaluation, the results demonstrate that MemVir is a flexible and powerful training strategy for many existing softmax variants and proxy-based losses.

CUB-200-2011 [28]											
T	Method	Net	Dim	R@1		R@2		R@4		R@8	
Ens	HDC [34]	G	384	53.6	-	65.7	-	77.0	-	85.6	-
	A-BIER [22]	G	512	57.5	-	68.7	-	78.3	-	86.2	-
	ABE [12]	G	512	60.6	-	71.5	-	79.8	-	87.4	-
Gen	DAML [3] + N-pair	G	512	52.7	-	65.4	-	75.5	-	84.3	-
	HDML [35] + N-pair	G	512	53.7	-	65.7	-	76.7	-	85.7	-
	Symm [5] + N-pair	G	512	55.9	-	67.6	-	78.3	-	86.2	-
	EE [15] + MS	G	512	57.4	-	68.7	-	79.5	-	86.9	-
	Symm [5] + MS	BN	512	64.9	-	76.4	-	84.6	-	90.5	-
	EE [15] + MS	BN	512	65.1	-	76.8	-	86.1	-	91.0	-
M	XBM [33] + Contrastive	BN	512	65.8	-	75.9	-	84.0	-	89.9	-
Pair	HTL [4]	BN	512	57.1	-	68.8	-	78.7	-	86.5	-
	RLL-H [32]	BN	512	57.4	-	69.7	-	79.2	-	86.9	-
	Multi-Similarity (MS)† [31]	BN	512	64.5	-	76.2	-	84.6	-	90.5	-
Softmax variant / Proxy	SoftTriple [24]	BN	512	65.4	-	76.4	-	84.5	-	90.4	-
	ProxyGML [36]	BN	512	66.6	-	77.6	-	86.4	-	-	-
	Circle [26]	BN	512	66.7	-	77.4	-	86.2	-	91.2	-
	Softmax	BN	512	64.2	-	75.7	-	84.1	-	89.9	-
	MemVir + Softmax	BN	512	66.8	(+2.6)	76.9	(+1.2)	85.4	(+1.3)	91.2	(+1.3)
	Norm-softmax [29]	BN	512	64.9	-	75.7	-	84.3	-	90.5	-
	MemVir + Norm-softmax	BN	512	67.3	(+2.4)	77.2	(+1.5)	85.3	(+1.0)	90.8	(+0.3)
	Cosface [30]	BN	512	65.7	-	76.2	-	84.7	-	90.6	-
	MemVir + Cosface	BN	512	67.7	(+2.0)	77.8	(+1.6)	85.7	(+1.0)	91.1	(+0.5)
	Arcface [2]	BN	512	66.1	-	76.6	-	84.8	-	90.7	-
	MemVir + Arcface	BN	512	67.4	(+1.3)	77.7	(+1.1)	85.5	(+0.7)	91.2	(+0.5)
	Proxy-NCA [19]	BN	512	64.3	-	75.3	-	83.6	-	89.6	-
	MemVir + Proxy-NCA	BN	512	68.3	(+4.0)	78.9	(+3.6)	85.7	(+2.1)	90.9	(+1.3)
	Proxy-anchor† [11]	BN	512	67.7	-	78.5	-	85.7	-	90.9	-
	MemVir + Proxy-anchor	BN	512	**69.0**	**(+1.3)**	**79.2**	**(+0.7)**	**86.8**	**(+1.1)**	**91.6**	**(+0.7)**
-	Average boost	-	-	-	(+2.3)	-	(+1.6)	-	(+1.2)	-	(+0.8)
	Minimum boost	-	-	-	(+1.3)	-	(+0.7)	-	(+0.7)	-	(+0.3)
	Maximum boost	-	-	-	(+4.0)	-	(+3.6)	-	(+2.1)	-	(+1.3)

Table E. **[Conventional evaluation]** Recall@k (%) on CUB-200-2011 dataset in image retrieval task. Method type (T) is denoted by abbreviations (*Ens*: ensemble, *Gen*: sample generation, *M*: memory-based, *Pair*: pair-based losses, *Softmax variant / Proxy*: softmax variants and proxy-based losses). Backbone network (Net) also is denoted by abbreviations (*G*: GoogleNet [27], *BN*: BN-Inception [9]). † denotes evaluation in a fair setting described in Section C.2.1.

CUB-200-2011 [28]	Concatenated (512-dim)			Separated (128-dim)		
Loss	P@1	RP	MAP@R	P@1	RP	MAP@R
Norm-softmax [29]	65.65 ± 0.30	35.99 ± 0.15	25.25 ± 0.13	58.75 ± 0.19	**31.75 ± 0.12**	**20.96 ± 0.11**
MemVir + Norm-softmax	**69.22 ± 0.15**	**37.92 ± 0.16**	**27.10 ± 0.13**	**59.83 ± 0.23**	31.46 ± 0.16	20.55 ± 0.14
CosFace [30]	67.32 ± 0.32	37.49 ± 0.21	26.70 ± 0.23	59.63 ± 0.36	31.99 ± 0.22	21.21 ± 0.22
MemVir + CosFace	**69.79 ± 0.26**	**37.85 ± 0.23**	**27.08 ± 0.28**	**61.33 ± 0.30**	**31.99 ± 0.18**	**21.30 ± 0.17**
ArcFace [2]	67.50 ± 0.25	37.31 ± 0.21	26.45 ± 0.20	60.17 ± 0.32	32.37 ± 0.17	21.49 ± 0.16
MemVir + ArcFace	**69.33 ± 0.41**	**37.82 ± 0.28**	**26.96 ± 0.25**	**61.38 ± 0.23**	**32.53 ± 0.13**	**21.58 ± 0.12**
Proxy-NCA [19]	65.69 ± 0.43	35.14 ± 0.26	24.21 ± 0.27	57.88 ± 0.30	30.16 ± 0.22	19.32 ± 0.21
MemVir + Proxy-NCA	**69.25 ± 0.32**	**37.31 ± 0.12**	**26.43 ± 0.17**	**60.08 ± 0.25**	**31.26 ± 0.15**	**20.30 ± 0.14**
Proxy-anchor [11]	69.73 ± 0.31	38.23 ± 0.37	27.44 ± 0.35	61.50 ± 0.34	32.94 ± 0.25	22.19 ± 0.25
MemVir + Proxy-anchor	**69.81 ± 0.28**	**38.57 ± 0.14**	**27.83 ± 0.16**	**62.58 ± 0.28**	**33.69 ± 0.18**	**22.75 ± 0.16**

Table F. **[MLRC evaluation]** Performance (%) on CUB-200-2011 dataset in image retrieval task. We report the performance of concatenated 512-dim and separated 128-dim. Bold numbers indicate the best score within the same loss.

CARS196 [16]											
T	Method	Net	Dim	R@1		R@2		R@4		R@8	
Ens	HDC [34]	G	384	73.7	-	83.2	-	89.5	-	93.8	-
	A-BIER [22]	G	512	82.0	-	89.0	-	93.2	-	96.1	-
	ABE [12]	G	512	85.2	-	90.5	-	94.0	-	96.1	-
Gen	DAML [3] + N-pair	G	512	75.1	-	83.8	-	89.7	-	93.5	-
	HDML [35] + N-pair	G	512	79.1	-	87.1	-	92.1	-	95.5	-
	Symm [5] + N-pair	G	512	76.5	-	84.3	-	90.4	-	94.1	-
	EE [15] + MS	G	512	76.1	-	84.2	-	89.8	-	93.8	-
	Symm [5] + MS	BN	512	82.4	-	89.2	-	93.3	-	96.1	-
	EE [15] + MS	BN	512	82.7	-	89.2	-	93.8	-	96.4	-
M	XBM [33] + Contrastive	BN	512	82.0	-	88.7	-	93.1	-	96.1	-
Pair	HTL [4]	BN	512	81.4	-	88.0	-	92.7	-	95.7	-
	RLL-H [32]	BN	512	74.0	-	83.6	-	90.1	-	94.1	-
	Multi-Similarity (MS)† [31]	BN	512	82.1	-	88.8	-	93.2	-	96.1	-
Softmax variant / Proxy	SoftTriple [24]	BN	512	84.5	-	90.7	-	94.5	-	96.9	-
	ProxyGML [36]	BN	512	85.5	-	91.8	-	95.3	-	-	-
	Circle [26]	BN	512	83.4	-	89.8	-	94.1	-	96.5	-
	Softmax	BN	512	81.5	-	89.0	-	93.6	-	96.8	-
	MemVir + Softmax	BN	512	86.5	(+5.0)	**92.4**	**(+3.4)**	**95.6**	**(+2.0)**	**97.4**	**(+0.6)**
	Norm-softmax [29]	BN	512	83.3	-	89.7	-	94.1	-	96.7	-
	MemVir + Norm-softmax	BN	512	**86.8**	**(+3.5)**	92.3	(+2.6)	95.4	(+1.3)	**97.4**	**(+0.7)**
	Cosface [30]	BN	512	83.6	-	89.9	-	94.2	-	96.6	-
	MemVir + Cosface	BN	512	86.6	(+3.0)	91.8	(+1.9)	95.1	(+0.9)	97.3	(+0.7)
	Arcface [2]	BN	512	83.7	-	90.0	-	94.3	-	96.8	-
	MemVir + Arcface	BN	512	86.5	(+2.8)	91.9	(+1.9)	95.1	(+0.8)	97.1	(+0.3)
	Proxy-NCA [19]	BN	512	82.0	-	89.2	-	93.8	-	96.4	-
	MemVir + Proxy-NCA	BN	512	86.5	(+4.5)	91.8	(+2.6)	95.5	(+1.7)	**97.4**	**(+1.0)**
	Proxy-anchor† [11]	BN	512	84.9	-	91.1	-	94.6	-	96.9	-
	MemVir + Proxy-anchor	BN	512	86.7	(+1.8)	92.0	(+0.9)	95.2	(+0.6)	**97.4**	**(+0.5)**
-	Average boost	-		-	(+3.4)	-	(+2.2)	-	(+1.2)	-	(+0.6
	Minimum boost	-		-	(+1.8)	-	(+0.9)	-	(+0.6)	-	(+0.3)
	Maximum boost	-		-	(+5.0)	-	(+3.4)	-	(+2.0)	-	(+1.0)

Table G. **[Conventional evaluation]** Recall@k (%) on CARS196 dataset in image retrieval task. Method type (T) is denoted by abbreviations (*Ens*: ensemble, *Gen*: sample generation, *M*: memory-based, *Pair*: pair-based losses, *Softmax variant / Proxy*: softmax variants and proxy-based losses). Backbone network (Net) also is denoted by abbreviations (*G*: GoogleNet [27], *BN*: BN-Inception [9]). † denotes evaluation in a fair setting described in Section C.2.1.

CARS196 [16]	Concatenated (512-dim)			Separated (128-dim)		
Loss	P@1	RP	MAP@R	P@1	RP	MAP@R
Norm-softmax [29]	83.16 ± 0.25	36.20 ± 0.26	26.00 ± 0.30	72.55 ± 0.18	29.35 ± 0.20	18.73 ± 0.20
MemVir + Norm-softmax	**85.81 ± 0.18**	**38.78 ± 0.19**	**28.92 ± 0.17**	**76.01 ± 0.23**	**30.86 ± 0.16**	**20.36 ± 0.16**
CosFace [30]	85.52 ± 0.24	37.32 ± 0.28	27.57 ± 0.30	74.67 ± 0.20	29.01 ± 0.11	18.80 ± 0.12
MemVir + CosFace	**87.57 ± 0.13**	**39.10 ± 0.21**	**29.56 ± 0.26**	**76.86 ± 0.28**	**30.59 ± 0.22**	**20.23 ± 0.24**
ArcFace [2]	85.44 ± 0.28	37.02 ± 0.29	27.22 ± 0.30	72.10 ± 0.37	27.29 ± 0.17	17.11 ± 0.18
MemVir + ArcFace	**88.02 ± 0.18**	**39.12 ± 0.15**	**29.63 ± 0.15**	**78.58 ± 0.26**	**31.03 ± 0.25**	**20.89 ± 0.26**
Proxy-NCA [19]	83.56 ± 0.27	35.62 ± 0.28	25.38 ± 0.31	73.46 ± 0.23	28.90 ± 0.22	18.29 ± 0.22
MemVir + Proxy-NCA	**87.02 ± 0.15**	**38.51 ± 0.15**	**28.76 ± 0.16**	**76.35 ± 0.28**	**30.29 ± 0.23**	**19.81 ± 0.25**
Proxy-anchor [11]	86.20 ± 0.21	39.08 ± 0.31	29.37 ± 0.29	76.97 ± 0.40	31.71 ± 0.53	21.29 ± 0.56
MemVir + Proxy-anchor	**86.40 ± 0.18**	**40.27 ± 0.20**	**30.58 ± 0.20**	**76.97 ± 0.26**	**32.87 ± 0.21**	**22.31 ± 0.22**

Table H. **[MLRC evaluation]** Performance (%) on CARS196 dataset in image retrieval task. We report the performance of concatenated 512-dim and separated 128-dim. Bold numbers indicate the best score within the same loss.

Stanford Online Products [21]											
T	Method	Net	Dim	R@1		R@10		R@100		R@1000	
Ens	HDC [34]	G	384	69.5	-	84.4	-	92.8	-	97.7	-
	A-BIER [22]	G	512	74.2	-	86.9	-	94.0	-	97.8	-
	ABE [12]	G	512	76.3	-	88.4	-	94.8	-	98.2	-
Gen	DAML [3] + N-pair	G	512	68.4	-	83.5	-	92.3	-	-	-
	HDM [35] + N-pair	G	512	68.7	-	83.2	-	92.4	-	-	-
	Symm [5] + N-pair	G	512	73.2	-	86.7	-	94.8	-	-	-
	EE [15] + MS	G	512	78.1	-	90.3	-	95.8	-	-	-
	Symm [5] + MS	BN	512	76.9	-	89.8	-	95.9	-	98.8	-
	EE [15] + MS	BN	512	77.0	-	89.5	-	96.0	-	98.8	-
M	XBM + Contrastive [33]	BN	512	79.5	-	90.8	-	96.1	-	98.7	-
Pair	HTL [4]	BN	512	74.8	-	88.3	-	94.8	-	98.4	-
	RLL-H [32]	BN	512	76.1	-	89.1	-	95.4	-	-	-
	Multi-Similarity (MS)† [31]	BN	512	76.3	-	89.7	-	96.0	-	98.8	-
Softmax variant / Proxy	SoftTriple [24]	BN	512	78.3	-	90.4	-	96.0	-	98.3	-
	ProxyGML [36]	BN	512	78.0	-	90.6	-	96.2	-	-	-
	Circle [26]	BN	512	78.3	-	90.5	-	96.1	-	98.6	-
	Softmax	BN	512	76.3	-	88.5	-	94.8	-	98.1	-
	MemVir + Softmax	BN	512	77.8	(+1.5)	89.8	(+1.3)	95.4	(+0.6)	98.4	(+0.3)
	Norm-softmax [29]	BN	512	78.6	-	90.5	-	96.0	-	98.6	-
	MemVir + Norm-softmax	BN	512	79.6	(+1.0)	90.9	(+0.4)	96.1	(+0.1)	98.7	(+0.1)
	Cosface [30]	BN	512	78.6	-	90.4	-	95.8	-	98.5	-
	MemVir + Cosface	BN	512	79.7	(+1.1)	90.5	(+0.1)	95.8	(0.0)	98.5	(0.0)
	Arcface [2]	BN	512	78.8	-	90.5	-	95.9	-	98.6	-
	MemVir + Arcface	BN	512	**80.0**	**(+1.2)**	90.9	(+0.4)	96.1	(+0.2)	98.7	(+0.1)
	Proxy-NCA [19]	BN	512	78.1	-	90.0	-	95.9	-	98.7	-
	MemVir + Proxy-NCA	BN	512	79.2	(+1.1)	90.4	(+0.4)	96.0	(+0.1)	**98.8**	**(+0.1)**
	Proxy-anchor† [11]	BN	512	78.9	-	90.6	-	96.1	-	98.5	-
	MemVir + Proxy-anchor	BN	512	79.7	(+0.8)	**91.0**	**(+0.4)**	**96.3**	**(+0.2)**	98.6	(+0.1)
-	Average boost	-	-	-	(+1.1)	-	(+0.5)	-	(+0.2)	-	(+0.1)
	Minimum boost	-	-	-	(+0.8)	-	(+0.1)	-	(0.0)	-	(0.0)
	Maximum boost	-	-	-	(+1.5)	-	(+1.3)	-	(+0.6)	-	(+0.3)

Table I. **[Conventional evaluation]** Recall@k (%) on Standford Online Products dataset in image retrieval task. Method type (T) is denoted by abbreviations (*Ens*: ensemble, *Gen*: sample generation, *M*: memory-based, *Pair*: pair-based losses, *Softmax variant / Proxy*: softmax variants and proxy-based losses). Backbone network (Net) also is denoted by abbreviations (*G*: GoogleNet [27], *BN*: BN-Inception [9]). † denotes evaluation in a fair setting described in Section C.2.1.

SOP [21]	Concatenated (512-dim)			Separated (128-dim)		
Loss	P@1	RP	MAP@R	P@1	RP	MAP@R
Norm-softmax [29]	75.67 ± 0.17	50.01 ± 0.22	47.13 ± 0.22	71.65 ± 0.14	45.32 ± 0.17	42.35 ± 0.16
MemVir + Norm-softmax	**75.77 ± 0.20**	**50.24 ± 0.22**	**47.45 ± 0.25**	**71.97 ± 0.15**	**45.47 ± 0.14**	**42.44 ± 0.14**
CosFace [30]	75.79 ± 0.14	49.77 ± 0.19	46.92 ± 0.19	**70.71 ± 0.19**	43.56 ± 0.21	40.69 ± 0.21
MemVir + CosFace	**75.88 ± 0.27**	**49.95 ± 0.37**	**47.18 ± 0.38**	70.25 ± 0.18	**43.82 ± 0.20**	**40.91 ± 0.19**
ArcFace [2]	**76.20 ± 0.27**	50.27 ± 0.38	47.41 ± 0.40	70.88 ± 1.51	44.00 ± 1.26	41.11 ± 1.22
MemVir + ArcFace	76.05 ± 0.30	**50.56 ± 0.33**	**47.75 ± 0.32**	**71.18 ± 0.27**	**44.31 ± 0.28**	**41.26 ± 0.28**
Proxy-NCA [19]	75.89 ± 0.17	50.10 ± 0.22	47.22 ± 0.21	71.30 ± 0.20	44.71 ± 0.21	41.74 ± 0.21
MemVir + Proxy-NCA	**76.97 ± 0.31**	**50.81 ± 0.26**	**48.02 ± 0.27**	**72.11 ± 0.25**	**44.82 ± 0.22**	**41.93 ± 0.18**
Proxy-ancho [11]	75.37 ± 0.15	50.19 ± 0.14	47.25 ± 0.15	71.56 ± 0.11	46.13 ± 0.21	43.03 ± 0.21
MemVir + Proxy-anchor	**77.80 ± 0.17**	**53.21 ± 0.12**	**50.35 ± 0.13**	**74.30 ± 0.18**	**48.94 ± 0.16**	**45.93 ± 0.15**

Table J. **[MLRC evaluation]** Performance (%) on Standford Online Products dataset in image retrieval. We report the performance of concatenated 512-dim and separated 128-dim. Bold numbers indicate the best score within the same loss.

References

[1] Jia Deng, Wei Dong, Richard Socher, Li-Jia Li, Kai Li, and Li Fei-Fei. Imagenet: A large-scale hierarchical image database. In *2009 IEEE conference on computer vision and pattern recognition*, pages 248–255. Ieee, 2009. vi

[2] Jiankang Deng, Jia Guo, Niannan Xue, and Stefanos Zafeiriou. Arcface: Additive angular margin loss for deep face recognition. In *Proceedings of the IEEE Conference on Computer Vision and Pattern Recognition*, pages 4690–4699, 2019. ii, xiv, xv, xvi

[3] Yueqi Duan, Wenzhao Zheng, Xudong Lin, Jiwen Lu, and Jie Zhou. Deep adversarial metric learning. In *Proceedings of the IEEE Conference on Computer Vision and Pattern Recognition*, pages 2780–2789, 2018. xiv, xv, xvi

[4] Weifeng Ge. Deep metric learning with hierarchical triplet loss. In *Proceedings of the European Conference on Computer Vision (ECCV)*, pages 269–285, 2018. xiv, xv, xvi

[5] Geonmo Gu and Byungsoo Ko. Symmetrical synthesis for deep metric learning. *arXiv preprint arXiv:2001.11658*, 2020. xiv, xv, xvi

[6] Kaiming He, Xiangyu Zhang, Shaoqing Ren, and Jian Sun. Deep residual learning for image recognition. In *Proceedings of the IEEE conference on computer vision and pattern recognition*, pages 770–778, 2016. x

[7] Yuge Huang, Yuhan Wang, Ying Tai, Xiaoming Liu, Pengcheng Shen, Shaoxin Li, Jilin Li, and Feiyue Huang. Curricularface: adaptive curriculum learning loss for deep face recognition. In *Proceedings of the IEEE/CVF Conference on Computer Vision and Pattern Recognition*, pages 5901–5910, 2020. iii, x

[8] Frank Hutter, Holger Hoos, and Kevin Leyton-Brown. An efficient approach for assessing hyperparameter importance. In *International conference on machine learning*, pages 754–762. PMLR, 2014. vii

[9] Sergey Ioffe and Christian Szegedy. Batch normalization: Accelerating deep network training by reducing internal covariate shift. *arXiv preprint arXiv:1502.03167*, 2015. vi, xiv, xv, xvi

[10] Alexander B. Jung, Kentaro Wada, Jon Crall, Satoshi Tanaka, Jake Graving, Christoph Reinders, Sarthak Yadav, Joy Banerjee, Gábor Vecsei, Adam Kraft, Zheng Rui, Jirka Borovec, Christian Vallentin, Semen Zhydenko, Kilian Pfeiffer, Ben Cook, Ismael Fernández, François-Michel De Rainville, Chi-Hung Weng, Abner Ayala-Acevedo, Raphael Meudec, Matias Laporte, et al. imgaug. https://github.com/aleju/imgaug, 2020. Online; accessed 01-Feb-2020. viii

[11] Sungyeon Kim, Dongwon Kim, Minsu Cho, and Suha Kwak. Proxy anchor loss for deep metric learning. *arXiv preprint arXiv:2003.13911*, 2020. ii, vi, xiv, xv, xvi

[12] Wonsik Kim, Bhavya Goyal, Kunal Chawla, Jungmin Lee, and Keunjoo Kwon. Attention-based ensemble for deep metric learning. In *Proceedings of the European Conference on Computer Vision (ECCV)*, pages 736–751, 2018. xiv, xv, xvi

[13] Yonghyun Kim, Wonpyo Park, and Jongju Shin. Broadface: Looking at tens of thousands of people at once for face recognition. *arXiv preprint arXiv:2008.06674*, 2020. viii, x

[14] Diederik P Kingma and Jimmy Ba. Adam: A method for stochastic optimization. *arXiv preprint arXiv:1412.6980*, 2014. vi, vii

[15] Byungsoo Ko and Geonmo Gu. Embedding expansion: Augmentation in embedding space for deep metric learning. In *Proceedings of the IEEE/CVF Conference on Computer Vision and Pattern Recognition*, pages 7255–7264, 2020. xiv, xv, xvi

[16] Jonathan Krause, Michael Stark, Jia Deng, and Li Fei-Fei. 3d object representations for fine-grained categorization. In *Proceedings of the IEEE international conference on computer vision workshops*, pages 554–561, 2013. vi, xv

[17] Ilya Loshchilov and Frank Hutter. Decoupled weight decay regularization. *arXiv preprint arXiv:1711.05101*, 2017. vii

[18] Laurens van der Maaten and Geoffrey Hinton. Visualizing data using t-sne. *Journal of machine learning research*, 9(Nov):2579–2605, 2008. xi

[19] Yair Movshovitz-Attias, Alexander Toshev, Thomas K Leung, Sergey Ioffe, and Saurabh Singh. No fuss distance metric learning using proxies. In *Proceedings of the IEEE International Conference on Computer Vision*, pages 360–368, 2017. ii, xiv, xv, xvi

[20] Kevin Musgrave, Serge Belongie, and Ser-Nam Lim. A metric learning reality check. *arXiv preprint arXiv:2003.08505*, 2020. vi

[21] Hyun Oh Song, Yu Xiang, Stefanie Jegelka, and Silvio Savarese. Deep metric learning via lifted structured feature embedding. In *Proceedings of the IEEE conference on computer vision and pattern recognition*, pages 4004–4012, 2016. vi, xvi

[22] Michael Opitz, Georg Waltner, Horst Possegger, and Horst Bischof. Deep metric learning with bier: Boosting independent embeddings robustly. *IEEE transactions on pattern analysis and machine intelligence*, 2018. xiv, xv, xvi

[23] Adam Paszke, Sam Gross, Francisco Massa, Adam Lerer, James Bradbury, Gregory Chanan, Trevor Killeen, Zeming Lin, Natalia Gimelshein, Luca Antiga, Alban Desmaison, Andreas Kopf, Edward Yang, Zachary DeVito, Martin Raison, Alykhan Tejani, Sasank Chilamkurthy, Benoit Steiner, Lu Fang, Junjie Bai, and Soumith Chintala. Pytorch: An imperative style, high-performance deep learning library. In H. Wallach, H. Larochelle, A. Beygelzimer, F. d'Alché-Buc, E. Fox, and R. Garnett, editors, *Advances in Neural Information Processing Systems 32*, pages 8024–8035. Curran Associates, Inc., 2019. vi

[24] Qi Qian, Lei Shang, Baigui Sun, Juhua Hu, Hao Li, and Rong Jin. Softtriple loss: Deep metric learning without triplet sampling. In *Proceedings of the IEEE International Conference on Computer Vision*, pages 6450–6458, 2019. vi, xiv, xv, xvi

[25] Kihyuk Sohn. Improved deep metric learning with multi-class n-pair loss objective. In *Advances in neural information processing systems*, pages 1857–1865, 2016. vi

[26] Yifan Sun, Changmao Cheng, Yuhan Zhang, Chi Zhang, Liang Zheng, Zhongdao Wang, and Yichen Wei. Circle loss: A unified perspective of pair similarity optimization. In *Proceedings of the IEEE/CVF Conference on Computer Vision and Pattern Recognition*, pages 6398–6407, 2020. xiv, xv, xvi

[27] Christian Szegedy, Wei Liu, Yangqing Jia, Pierre Sermanet, Scott Reed, Dragomir Anguelov, Dumitru Erhan, Vincent Vanhoucke, and Andrew Rabinovich. Going deeper with convolutions. In *Proceedings of the IEEE conference on computer vision and pattern recognition*, pages 1–9, 2015. xiv, xv, xvi

[28] Catherine Wah, Steve Branson, Peter Welinder, Pietro Perona, and Serge Belongie. The caltech-ucsd birds-200-2011 dataset. 2011. vi, xiv

[29] Feng Wang, Xiang Xiang, Jian Cheng, and Alan Loddon Yuille. Normface: L2 hypersphere embedding for face verification. In *Proceedings of the 25th ACM international conference on Multimedia*, pages 1041–1049, 2017. xiv, xv, xvi

[30] Hao Wang, Yitong Wang, Zheng Zhou, Xing Ji, Dihong Gong, Jingchao Zhou, Zhifeng Li, and Wei Liu. Cosface: Large margin cosine loss for deep face recognition. In *Proceedings of the IEEE Conference on Computer Vision and Pattern Recognition*, pages 5265–5274, 2018. ii, xiv, xv, xvi

[31] Xun Wang, Xintong Han, Weilin Huang, Dengke Dong, and Matthew R Scott. Multi-similarity loss with general pair weighting for deep metric learning. In *Proceedings of the IEEE Conference on Computer Vision and Pattern Recognition*, pages 5022–5030, 2019. vi, vii, xiv, xv, xvi

[32] Xinshao Wang, Yang Hua, Elyor Kodirov, Guosheng Hu, Romain Garnier, and Neil M Robertson. Ranked list loss for deep metric learning. In *Proceedings of the IEEE Conference on Computer Vision and Pattern Recognition*, pages 5207–5216, 2019. xiv, xv, xvi

[33] Xun Wang, Haozhi Zhang, Weilin Huang, and Matthew R Scott. Cross-batch memory for embedding learning. In *Proceedings of the IEEE/CVF Conference on Computer Vision and Pattern Recognition*, pages 6388–6397, 2020. iv, viii, x, xiv, xv, xvi

[34] Yuhui Yuan, Kuiyuan Yang, and Chao Zhang. Hard-aware deeply cascaded embedding. In *Proceedings of the IEEE international conference on computer vision*, pages 814–823, 2017. xiv, xv, xvi

[35] Wenzhao Zheng, Zhaodong Chen, Jiwen Lu, and Jie Zhou. Hardness-aware deep metric learning. In *Proceedings of the IEEE Conference on Computer Vision and Pattern Recognition*, pages 72–81, 2019. xiv, xv, xvi

[36] Yuehua Zhu, Muli Yang, Cheng Deng, and Wei Liu. Fewer is more: A deep graph metric learning perspective using fewer proxies. *arXiv preprint arXiv:2010.13636*, 2020. vii, xiv, xv, xvi